수의학석사학위논문

아밀로이드 베타(Aβ)의 미토콘드리아 분절을 통한 신경세포 자멸사에서 Akt-Drp1 활성화의 역할

Amyloid β-Induced Drp1 Phosphorylation through Akt Activation Promotes Excessive Mitochondrial Fission Leading Neuronal Apoptosis

2016년 8월

서울대학교 대학원

수의학과 수의생명과학 전공

김 다 임

ABSTRACT

Amyloid β-Induced Drp1 Phosphorylation through Akt Activation Promotes Excessive Mitochondrial Fission Leading Neuronal Apoptosis

Dah Ihm Kim

Major in Veterinary Biomedical Science

Department of Veterinary Medicine

The Graduate School

Seoul National University

Mitochondrial dysfunction is known as one of causative factors in Alzheimer's disease (AD), inducing neuronal cell death. Mitochondria regulate their functions through changing their morphology. The present work was undertaken to investigate whether Amyloid β (Aβ) affects mitochondrial morphology in neuronal cells inducing apoptosis. Aβ treatment induced not only the

fragmentation of mitochondria but also the neuronal apoptosis in a dose-dependent manner in association with increase in caspase-9 and -3 activities. My work showed that the mitochondrial dymamics are highly dependent on the concentration of Aβ. Calcium influx induced by Aβ up-regulated the activation of Akt through CaMKII, resulted in the phosphorylation level of Drp1 in a time-dependent manner. Translocation of Drp1 from cytosol to mitochondria was blocked by Akt inhibitor. Recruitment of Drp1 on the mitochondria lead to ROS generation by mitochondrial fission which induce the dysfunction of mitochondria such as loss of membrane potential and ATP production. ROS generation and mitochondrial dysfunction by Aβ were attenuated, when treated with mdivi-1, selective Drp1 inhibitor. Furthermore, the sustained Akt activation induced not only the fragmentation of mitochondria but also the activation of mTOR, eventually suppressing the autophagy. Inhibition of autophagic clearance by Aβ lead to the increase of ROS level and the worsening defect of mitochondria, which was blocked by Rapamycin (an mTOR inhibitor). In conclusion, sustained phosphorylation of Akt by Aβ directly activated Drp1, as well as autophagy inhibition through mTOR pathway. These elicited the abundant mitochondrial

fragmentation resulting in ROS-mediated neuronal apoptosis.

Keywords: Amyloid β (Aβ), Mitochondrial dynamics, Akt, CaMKII, Drp1, ROS, Autophagy

Student Number: 2014-21926

CONTENTS

LIST OF FIGURES

LIST OF TABLE

ABBREVIATIONS

NAC	N-acetyl-L-cysteine
ATP	Adenosine triphosphate
ETC	Electron transport chain
Drp1	Dynamin-related protein
Fis1	mitochondrial fission protein1
Mfn1/2	mitofusin1/2
Opa1	Optic atrophy1
NMDAR	N-methyl-D-aspartate receptor
CaMKII	Calmodulin-dependent kinaseII
CaM	Calmodulin
L-VGCC	L-type voltage-gated calcium channel
Akt	Protein kinase B
FITC	Fluorescein isothiocyanate
DMEM	Dulbecco Modified Eagle Medium
PBS	Phosphate buffered solution
FBS	Fetal bovine serum
NGS	Normal goat serum
HFIP	1,1,1,3,3,3,-hexafluoro-2-propanol

RT	Room temperature
AraC	Cytosine arabinoside
PCR	Polymerase chain reaction
PVDF	Polyvinylidene fluoride

INTRODUCTION

Alzheimer's disease (AD), characterized by memory deficits and cognitive impairments, is one of the most common types of age-related brain disorders causing dementia. Because it has the highest toxicity towards neuronal functions, amyloid β (Aβ) has been considered as a major risk factor of AD [1]. Aβ leads to neuronal cell death which is one of the major hallmarks of AD including abnormal mitochondria, neurofibrillary tangle (NFT) and amyloid plaques [2] [3]. Accumulation of dysfunctional mitochondria is frequently observed in the brains of AD patients [4] [5]. Neuronal cells require much energy and are reliant on proper mitochondrial function. Many studies have focused on mitochondria as a significant controller in neurodegenerative diseases due to their regulation role in cell fate and energy generation of a cell. Consequently, maintaining the function of mitochondria became a therapeutic target of AD pathogenesis [6] [7].

The function of mitochondria is tightly related with their morphology transition by fusion and fission. An imbalance of

mitochondrial dynamics causes the accumulation of fragmented mitochondria and impairs their function [8]. Defects in mitochondria, such as impairment of the electron transport chain (ETC), lead to ATP depletion and ROS generation which are correlated with fragmented mitochondria often found in the brains of AD patients [9] [10]. Five key molecules are known to control mitochondrial dynamics: dynamin-related protein 1 (Drp1), mitochondrial fission protein 1 (Fis1), mitofusin 1/2 (Mfn 1/2) and optic atrophy (Opa1) [11] [12]. Both the expression levels and post-translational modifications of mitochondrial dynamic proteins are regulated in many ways including controlling protein interactions, localizations, and activations. Post-translational modification by phosphorylation of Drp1 on serine residues regulates its downstream signal which subsequently affects the fragmentation of mitochondria [13]. Modification of fission proteins, primarily through phosphorylation, not only induces mitochondrial fission but also affects their function. A recent study investigated how mitochondrial fusion and fission generally occurs. Mitochondrial fission is closely related with mitosis and neuronal excitation. Linkage of excessive mitochondrial fragmentation and altered signals in AD patients suggest cyclin-

dependent kinase (CDK) and calcium associated signal as one of the Drp1 regulators [14] [15]. Establishing a fission regulatory pathway could help to overcome the imbalance of mitochondrial dynamics in several neurodegenerative diseases such as AD. However, the precise mechanism of Aβ-induced mitochondria fragmentation causing the progression of AD remains unclear. This prompted us to find the upstream signal molecule regulating mitochondrial fragmentation.

Several in vitro models in human neuroblastoma (NB) cell-lines (SK-N-MC, SK-N-SH, SH-SY5Y) and mouse hippocampal neurons were used in this experiment to examine the mechanism of Aβ-induced mitochondrial alteration. NB were used to investigate Aβ-induced mitochondrial dynamics as an in vitro model for AD. The NB cell-line has three different phenotypes: neuroblastic N-type cells, substrate-adherent S-type cells, and intermediate I-type cells. To ensure that the response of Aβ stimulation is not from the different phenotypes of the NB cell-line, SH-SY5Y and its parental line SK-N-SH to represent the N- and S- type cells and the SK-N-MC for the I-type of the NB cells were used. Furthermore, because of its similarity to an in vivo model, primary mouse

hippocampal neurons were compared with the human cell-line to confirm that they respond in the same manner after Aβ treatment. Aβ-induce Drp1 phosphorylation leading to mitochondrial fission has been implicated in many studies. In the present study, I investigated the signaling pathway that cause both mitochondrial fission and abnormal mitochondrial accumulation which eventually triggers neuronal apoptosis.

MATERIALS AND METHODS

1. Materials

Human neuroblastoma cell lines were obtained from Korean Cell Line Bank (Seoul, Korea). Fetal bovine serum (FBS) was purchased from Bio Whittaker (Walkersville, MD, USA). Antibodies specific for Mfn 2, Opa1, Drp1, Fis1, Caspase 3, Caspase 9, p-AKT (Ser 473), AKT, p-CaMKII (Thr 286), CaMKII, CaM, mTOR, Cyt C, Bax, Bcl-2, COX IV, β-tubulin, and β-actin were aquired from Santa Cruz Biotechnology (Santa Cruz, CA, USA). p-Drp1 (Ser 616), p-mTOR (Ser 2448) antibodies were purchased from Cell Signaling Technology, Inc. (Danvers, MA, USA). The antibodies of LC3 and p62 were obtained from Novus Biologicals (Littleton, CO, USA). Mfn 1 antibody was purchased from Proteintech (Wuhan, China). Horseradish peroxidase (HRP)-conjugated IgG was obtained from Jackson Immunoresearch (West Groove, PA, USA). EGTA, Ionomycin, Nifedipine, MK-801, NAC, Rapamycin, Trehalose and 3-MA was purchased from Sigma Chemical Company (St. Louis, MO,

USA). mdivi-1 was purchased from Enzo life sciences (Farmingdale, NY, USA). AKT inhibitor was purchased from Calbiochem (La Jolla, CA, USA).

2. Cell culture

Three different human neuroblastoma cell lines were used: SK-N-MC, SK-N-SH and SHSY-5Y were used. Cells were cultured in Dulbecco Modified Eagle Medium (DMEM; Thermo Fisher) supplemented with 1% antibiotics and 10% FBS. Cells were grown in 35, 60, or 100 mm diameter culture dishes, or in 12- or 96-well plate at 37° C with 5% CO_2 in the incubator. Cells were transferred to serum-free medium. After 24h incubation, cells were cultured at 70-80% confluence, and were transferred to serum-free medium prior to experiments.

3. Primary culture of mouse hippocampal neurons

Prenatal mice (18-19 days) were used to isolate hippocampal primary neurons. Isolated hippocampi were minced gently using a sterile scalpel, and treated with trypsin (0.025%). 2.5×10^6 cells

were plated at poly-D-lysine coated 35 mm dish in Neurobasal Plating Media (Neurobasal Media containing B27 Supplement [1ml/50ml], 0.5mM Glutamine Solution, 25 μM Glutamate, 0.5 % antibiotics, 1mM HEPES, 10 % Heat Inactivated Donor Horse Serum) and placed in an incubator at 37° C with 5% CO_2. After 24 hours, growth media was changed to Neurobasal Feeding Media (Neurobasal Media containing B27 Supplement [1ml/50ml], 0.5mM Glutamine Solution, 0.5% antibiotics, 1 mM HEPES. Cytosine arabinoside (AraC) was treated to avoid glial cell early time points in the culture. NeuN was purchased from Abcam (Cambridge, England) and used for staining neurons' nuclear.

4. Aβ oligomerization

The β-Amyloid [1-42] (Human) peptide was purchased from Invitrogen Corporation (Camarillo, CA, USA). 1 mg of the peptide was dissolved in 1 ml of a 100% HFIP (1,1,1,3,3,3,-hexafluoro-2-propanol [Sigma Chemical Company (St. Louis, MO, USA)]). Then incubated for 1 hour in Room Temperature and occasionally vortexed. Sonication for 10 minutes in a water bath and then freeze-dried for

3 hours. After the film formation, peptide were dissolved in 100% DMSO (1 mM). PBS (100 μM) was added for dilution, and then incubated for 24 hours at 4° C to oligomerize Aβ.

5. Real Time quantitative PCR

Total RNA of SK-N-MC was extracted by using MiniBEST Universal RNA Extraction Kit (TaKaRa, Otsu, Shinga, Japan) according to the manufacturer's instructions. Reverse transcription was carried out using 1 μg of RNA by MaximeTM RT-PCR PreMix kit (iNtRON, Seongnam, Korea) with the oligo(dT)18 primers under the conditions: cDNA synthesis at 45° C for 60 min, and RTase inactivation at 95° C for 5 min. Real Time quantification of RNA targets were performed using Rotor-Gene 6000 thermal cycling system(Corbett Research, Cambridge, UK) with a QuantiSpeed SYBR Kit (PKT). The cDNA was amplified by PCR premix kit (iNtRON) under the conditions : denaturation at 94° C for 5 min, 40 cycles at 94° C for 15 sec, annealing temperature (AT) for 20 sec, and 72 ° C for 30 sec using MyGenie™ 96 Thermal Block (Bioneer, Daejeon, Korea). Human primer sequences for reactions are listed in

Supplementary Table 1. Data analysis was performed using the software provided.

6. Western blotting

Cells were washed twice with cold PBS followed by incubation in lysis buffer (20 mM Tris [pH 7.5], 1 mM EDTA, 1 mM EGTA, 1 % Triton X-100, 1 mg/ml aprotinin, 1 mM PMSF, and 0.5 mM sodium orthovanadate) for 30 min on ice. The pre-cleared lysates were centrifuged at 15000 rpm at 4° C for 30 min, and then determined protein concentration by BCA protein assay. Samples containing 15 μg of protein were resolved by sodium dodecyl sulfate-polyacrylamide gel electrophoresis (SDS-PAGE) and transferred to a polyvinylidene fluoride (PVDF) membrane. The membranes were washed with tris-buffered saline containing 0.1% Tween-20 (TBST) solution [10mM Tris-HCL (pH 7.6), 150 mM NaCl, and 0.1% Tween-20] and blocked with 5% skim milk for 30 min. The membranes were washed with TBST for 3 times every 10 min, and were incubated with the primary antibody at 4° C for overnight. After incubation, the membranes were washed and then incubated with

HRP-conjugated secondary antibody at 4° C for 4 hours. The specific bands were visualized by using ChemiDoc™ XRS+ System (Bio-Rad, Richmond, CA). Densitometric analysis was carried out by using Image J software. Each of protein phosphorylation and expression was normalized by β-actin.

7. Calcium imaging

Fluo 3-AM(2 μM) was used to detect the intracellular calcium levels. The cells were plated on confocal dishes and were washed with a PBS once. The cells were then incubated in PBS containing 3 μM Fluo 3-AM with 5% CO2 at 37° C for 40 minutes. The cells were imaged using laser confocal microscopy (X400) (Fluo View 300) with an excitation wavelength of 488 nm and an emission wavelength of 515 nm. Ionomycin was applied as a positive control. Analysis of intracellular calcium levels processed at a single cell level are expressed as the relative fluorescence intensity (RFI).

8. Mitochondria morphology

To visualize mitochondria, the cells were cultured in confocal dish and incubated with Mitotracker Green FM (200 nM) for 30 min at 37° C. After incubation, the cells were washed twice with pre-warmed DMEM. The analysis was performed using laser confocal microscopy (X400) (Fluo View 300) with an excitation wavelength of 488 nm and an emission wavelength of 500 nm. To quantify mitochondrial morphology, 10 regions with more than 30 cells were randomly chosen and classified into three categories (tubular, intermediate, fragmented) depending on mitochondrial length. Each category was quantified as percentage.

9. Measurement of ROS

CM-H_2DCFDA (DCF-DA), a fluorescence-based probe, was used to detect intracellular Reactive oxygen species (ROS). The cells were plated on 96 well dish and then incubated with 10 μM DCF-DA in dark for 30 min at room temperature. Intracellular hydrogen peroxide (H_2O_2) levels were assessed by luminometer (Victor3,

Perkin-Elmer, Waltham, MA). Normalization was performed by dividing the total cell numbers.

10. Measurement of cellular ATP levels

ATP Bioluminscent HSII kit (Roche) was used to measure intracellular ATP concentration from cells according to the manufacturer's instructions. Briefly, cells were boiled in lysis buffer for 5 min at 100° C, followed by centrifugation for 2 min at 15,000 r.p.m. The supernatant was collected and placed on ice. Same volume of extract and luciferase reagent were injected in a 96-well black-walled with clear-bottomed plate. ATP concentrations were normalized to total protein concentration.

11. Mitochondrial membrane potential

Cells were cultured in confocal dish, and then stained with cationic dye JC-1 (2.5 μM) with 5% CO_2 at 37° C for 20 min. The cells were imaged using laser confocal microscopy (X400) (Fluo View 300) with an excitation wavelength of 488 nm and an emission wavelength of

590 nm. JC-1 monomer produces a green fluorescence at low membrane potentiasl while aggregation of JC-1 produces a red fluorescence at intact membrane potentials.

12. Immunocytochemistry

Cells were cultured in confocal dish, and then were fixed with 4% paraformaldehyde (Sigma-Aldrich) for 10 min. 0.1% Triton X-100 diluted in PBS was used for permeabilization for 5 min. 1% NGS was used to decrease non-specific binding of antibody for 30 min, and then incubatied with 1:100 dilution of primary antibody for overnight at 4° C. Next, the cells were incubated with either fluorescein isothiocyanate (FITC) conjugated anti-rabbit and anti-mouse IgG antibody (1:200) in dark for 1 h in RT. Next, representative images were obtained by FluoView™ 300 fluorescence microscope (Olympus, Tokyo, Japan).

13. Co-immunoprecipitation

The complex formation between proteins analyzed by

immunoprecipitation and Western blot. Cells were lysed with the co-immunoprecipitation (IP) buffer (1% Triton X-100 in 50mM Tris-HCl [pH 7.4] containing 150 mM NaCl, 5 mM EDTA, 2 mM NA_3VO_4, 2.5 mM Na_4PO_7, 100 mM NaF, 200 nM microcystin lysin-arginine, and protease inhibitor). Cell lysates (400 μg) were mixed with 10 μg of anti-CaMKII or Akt antibodies. The cell lysates were incubated for 4h at 4° C, and Protein A/G PLUS-agarose IP reagent (Pierce; Rockford, IL, USA) was added. After additional incubation for 12 h, the beads were washed three times with the co-IP buffer, and the bound proteins were eluted by boiling in sodium dodecylsulfate-polyacrylamide gel electrophoresis (SDS-PAGE) sample buffer for 5 min. Samples were analyzed by western blotting with CaM, CaMKII, Akt, and Drp1 antibodies.

14. Cytosol and mitochondria fractionation

Isolation of the mitochondrial fraction was performed using mitochondria extraction kit in cells (Thermo Fisher Scientific, Rockford, IL). Cytoplasmic and mitochondrial proteins were extracted from cells according to the manufacturer's instructions.

Briefly, cells were washed with cold PBS and then collected using a scraper. After centrifugation, cells were lysed in 400 μL mitochondria isolation buffer. After centrifugation, nuclei and unbroken cells were removed and the supernatants were centrifuged to obtain the pellet (mitochondria).

15. Detection of neuronal apoptosis

Annexin V / propidium iodide (PI) staining kit (BD Biosciences) was used to detect neuronal apoptosis. Cells were detached by 0.05% trypsin/EDTA and resuspended with Annexin V binding buffer. 1 × 10^5 cells were taken for staining, and then incubated with Annexin V and PI and for 20 min at room temperature in the dark. Cells were analyzed by flow cytometry using CXP software (Beckman Coulter, Brea, CA).The debris is excluded from the gates (forward light scatter [FSC] area versus side scatter area), and then any cell doublets were excluded using FSC area versus FSC width analysis. Trypan blue exclusion assay to evaluate cell viability was performed in cells in a 12-well plate. Cells were detached by 0.05 % Trypsin and 0.5mM EDTA solution and then treated with soybean trypsin

inhibitor (0.05 mg/mL). The cells were added with 0.4 % trypan blue and were counted by using a Petroff-Hausser counting chamber. Cell viability = {1- (number of trypan blue-stained cell ÷ number of total cells) × 100}.

16. Statistical analysis

Results are expressed as mean ± standard error of mean (SEM). All results were analyzed by ANOVA, and BonferroniDunn test was used to compare multiple experiments. p-value of < 0.05 was considered statistically significant.

RESULTS

1. Effect of Aβ on mitochondria dynamics

The effect of Aβ on mitochondrial dynamics in neuronal cells was evaluated by the morphological alterations in the mitochondria which were stained with Mitotracker Green and observed by laser confocal microscopy. For the determination of fission and fusion, the mitochondrial length was classified into three categories: >3 μm, 1–3 μm, and <1 μm. Mitochondria morphology in SK–N–MC treated with 5 μM Aβ was changed from a tubular shape at the initial stages to a fragmented shape (45%) (Figure 1A). Moreover, Aβ–induced alterations in mitochondria were also revealed in the other subtypes of neuroblastoma cell lines SK–N–SH and SH–SY5Y and in the mouse hippocampal primary neurons. Mitochondrial fission by Aβ increased with time, showing a significantly round morphology at 48 hours in neural cell lines. Also, Aβ attenuated mitochondrial network continuity in primary neurons (Figure 1B). Consequently, 5 μM Aβ

for 48 hours was used for further investigation in my study to examine how Aβ oligomer alters the morphology of mitochondria. Pretreatment of Mdivi-1 (Mitochondrial fission inhibitor) with Aβ decreased the cleavage of caspase 9 and 3 in neural cell lines (Figure 1C). The trypan blue assay showed that the rate of Aβ-induced apoptotic cells was reversed by Mdivi-1 pretreatment (Figure 1D). Moreover, Aβ increased the rate of late apoptosis (25±0.33%) compared with the control (10±0.69%). In contrast, Mdivi-1 decreased the rate of apoptosis, supporting that Aβ-induced mitochondrial fission leads to neuronal apoptosis (Figure 1E).

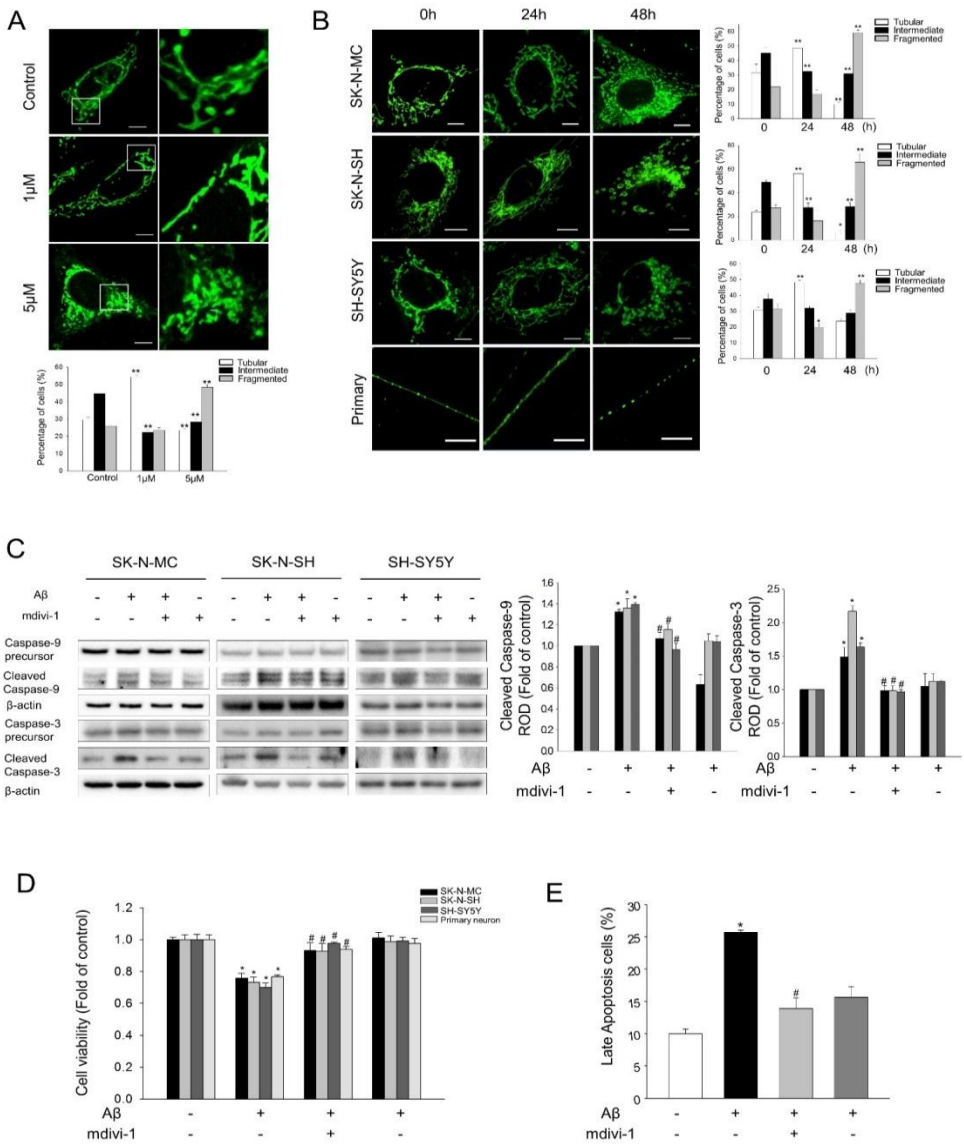

Fig. 1 Effect of Aβ on mitochondrial dynamics in neuronal cells. (A) SK-N-MC cells were exposed to Aβ at the indicated concentrations for 48h and then loaded with MitoTracker Green (200 nM). Representative images were obtained by confocal microscopy. The individual mitochondrial length was assessed and classified into three different categories and quantified as percentage. Data represent mean ±

SEM of ten random fields from three experiments for each condition. Scale bar, 5 μm. **p<0.01 versus control. (B) Three different neuronal cell lines and primary neurons were treated with 5 μM Aβ for various time and then loaded with MitoTracker Green (200 nM). Representative images were obtained by confocal microscopy. The individual mitochondrial length was assessed and classified into three different categories and quantified as percentage. Data represent mean ± SEM of ten random fields from three experiments for each condition. Scale bar, 5 μm. *p<0.05 versus control, **p<0.01 versus control. (C) Three different neuronal cell lines were pretreated with/without Mdivi-1 (1 μM) for 30 min, and then exposed to Aβ (5 μM) for 48 h. The cell lysates were subjected to western blotting, and determined by caspase-9 and caspase-3 antibodies. The bars in the below part of panel denote mean ± SEM of three experiments for each condition determined by densitometry relative to total protein. *p<0.05 versus control, #p<0.05 versus Aβ. (D) Cells were pre-treated with/without Mdivi-1(1 μM) for 30 min, and then exposed to Aβ (5 μM) for 48 h. Cell viability for SK-N-MC cells and primary neurons were measured by Trypan blue exclusion assay. Data represent mean ± SEM. n=5. *p<0.05 versus control, #p<0.05 versus Aβ. (E) Quantitative analysis of the fold changes of late apoptotic cells were measured by using annexin V/proidium iodide (PI) staining. SK-N-MC cells were pretreated with/without Mdivi-1 (1 μM) and then, exposed to 5 μM Aβ for 48 h. The cells were stained with Annexin V (25 μg/ml) and PI (125 ng/ml), and incubated for 30min at room temperature in the dark and quantified by flow cytometry. Data represent mean ± SEM. n=5. *p<0.05 versus control, #p<0.05 versus Aβ.

2. Aβ induces Drp1 dependent mitochondrial fission through sustained Akt activation

Extracellular calcium influx was blocked both by MK-801 (NMDAR antagonist) and nifedipine (L-type blocker), indicating that Aβ induced high levels of voltage-dependent calcium influx (Figure 2A). Calmodulin-dependent protein kinase II (CaMKII), phosphorylated by Aβ, showed a significant increase with time after 15 min. (Figure 2B). Aβ increased the affinity of Ca^{2+}-carried Calmodulin (CaM) and CaMKII (Figure 2C). Moreover, activation of CaMKII Thr 286, which was increased by Aβ, was blocked by EGTA (Extracellular calcium chelator), suggesting that Aβ-induced calcium influx regulates the CaMKII activity (Figure 2D). To confirm that calcium influx affect Akt activation, KN-93 which are inhibitor of CaMKII was used. The Aβ-induced Akt phosphorylation levels were attenuated by KN-93 (Figure 2E). CaMKII activation through Aβ-induced calcium influx directly increased Akt binding and regulated its activity. The CaMKII and Akt binding interaction was suppressed by KN-93 (Figure 2F).

Because mitochondrial fission occurs during cell proliferation, I determined whether there is a relationship between dynamic proteins in the mitochondria and cell proliferation associated proteins. Akt phosphorylation at Ser473 showed an increase with time especially 3 hours after the Aβ treatment (Figure 3A). Cells treated with Aβ had significantly increased binding interaction between Akt and Drp1 when compared to the control (Figure 3B). Moreover, confocal microscopy studies showed a great increase in the co-localization of Akt and Drp1 (Figure 3C). The Aβ-induced Drp1 phosphorylation levels of Ser616, an activated form of Drp1 leading to mitochondrial fission, were blocked by the Akt inhibitor in both human neuronal cell lines and primary neurons (Figure 3D). These results suggest that the activated Akt directly binds to Drp1, facilitating the increased levels of phosphorylation on the Ser616 sites. Aβ treatment increased the translocation of Drp1 from the cytosol to mitochondria, which was blocked by the Akt inhibitor, suggesting that Aβ-induced Drp1 oligomerization occurred through translocation of Drp1 to mitochondria (Figure 3E). Aβ-induced mitochondrial fission was confirmed with Mdivi-1 by preventing it, suggesting that Akt activation by Aβ phosphorylates directly Drp1 leading to the fission

of mitochondria (Figure 3F).

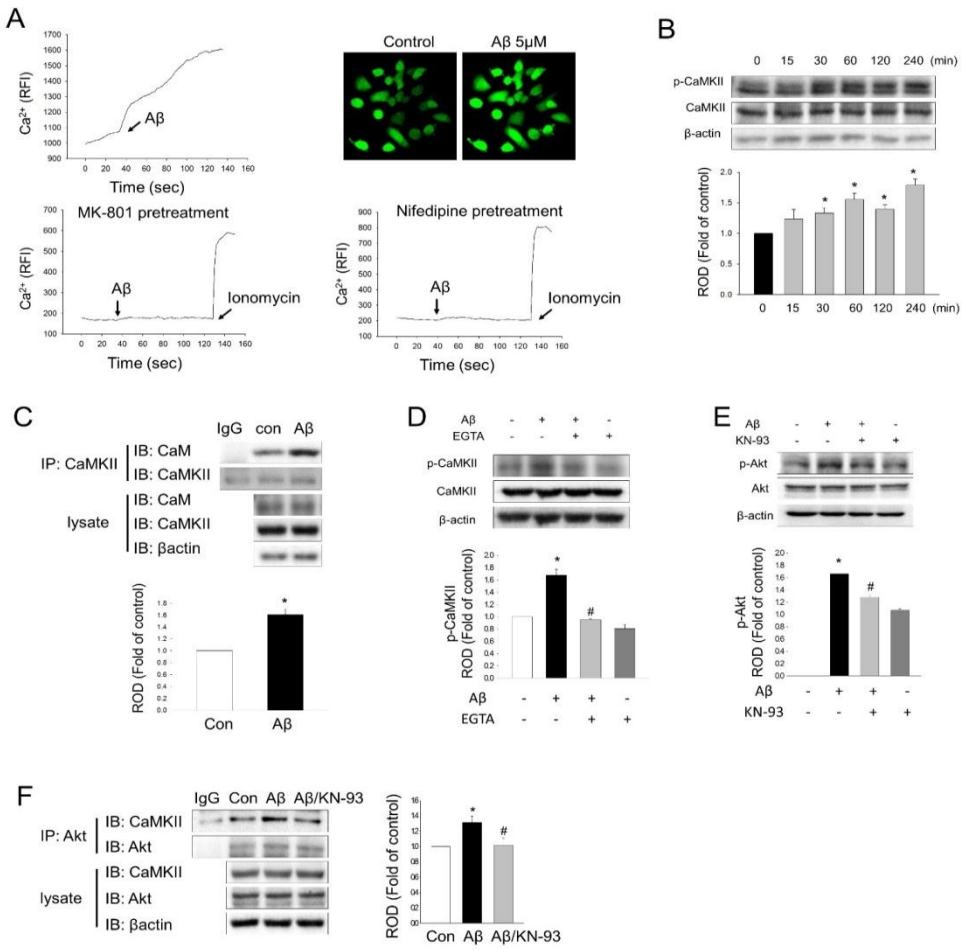

Fig. 2 Aβ induced calcium influx activates aberrant Akt signaling pathway. (A) SK-N-MC cells were loaded with Fluo 3-AM (2 μM) for 30 mins and pretreated with MK-801 (10 μM) and Nifedipine (10 μM) for 30 min and then exposed to Aβ (5 μM). Alteration of Ca2+ was measured using confocal microscopy. Ionomycin (2 μM) was treated as positive control. n=3. (B) SK-N-MC cells were treated with 5 μM Aβ for 0-240 min. Total cell lysates were subjected to western blotting and phospho-CaMKIIThr286 and CaMKII expression levels were detected. The bars in

the below panel denote mean ± SEM of three experiments for each condition determined by densitometry relative to total-CaMKII and to the loading control β-actin. *p<0.05 versus 0 h. (C) SK-N-MC cells treated with Aβ for 30 min prior to harvesting. CaMKII protein was co-immunoprecipitated with CaM and analyzed by western blotting (up). Expression of CaM and CaMKII in total cell lysates is shown (down). n=3 *p<0.05 versus control. (D) SK-N-MC cells were pretreated with/without EGTA (1 mM) for 30 min, and then exposed to Aβ (5 μM) for 1 h. The cell lysates were subjected to western blotting, and determined by phospho-CaMKIIThr286 and CaMKII antibodies. The bars in the below part of panel denote mean ± SEM of three experiments for each condition determined by densitometry relative to total-CaMKII and to the loading control and to the loading control β-actin. *p<0.05 versus control, #p<0.05 versus Aβ. (E) SK-N-MC cells were pretreated with/without KN-93 (1 μM) for 30 min, and then exposed to Aβ (5 μM) for 3 h. The cell lysates were subjected to western blotting, and determined by phospho-AktTer473 and Akt antibodies. The bars in the below part of panel denote mean ± SEM of three experiments for each condition determined by densitometry relative to total-AKT and to the loading control β-actin protein. *p<0.05 versus control, #p<0.05 versus Aβ. (F) SK-N-MC cells were pretreated with/without KN-93 (1 μM) for 30 min, and then exposed to Aβ for 3h prior to harvesting. Akt protein was co-immunoprecipitated with CaMKII. Cells were subjected to precipitation by Akt antibody. The precipitated complex was analyzed by western blotting and detected with CaMKII antibody (up). Expression of CaMKII and Akt in total cell lysates is shown (down). n=3, *p<0.05 versus control. IP: Immunoprecipitation, IB: Immunoblotting.

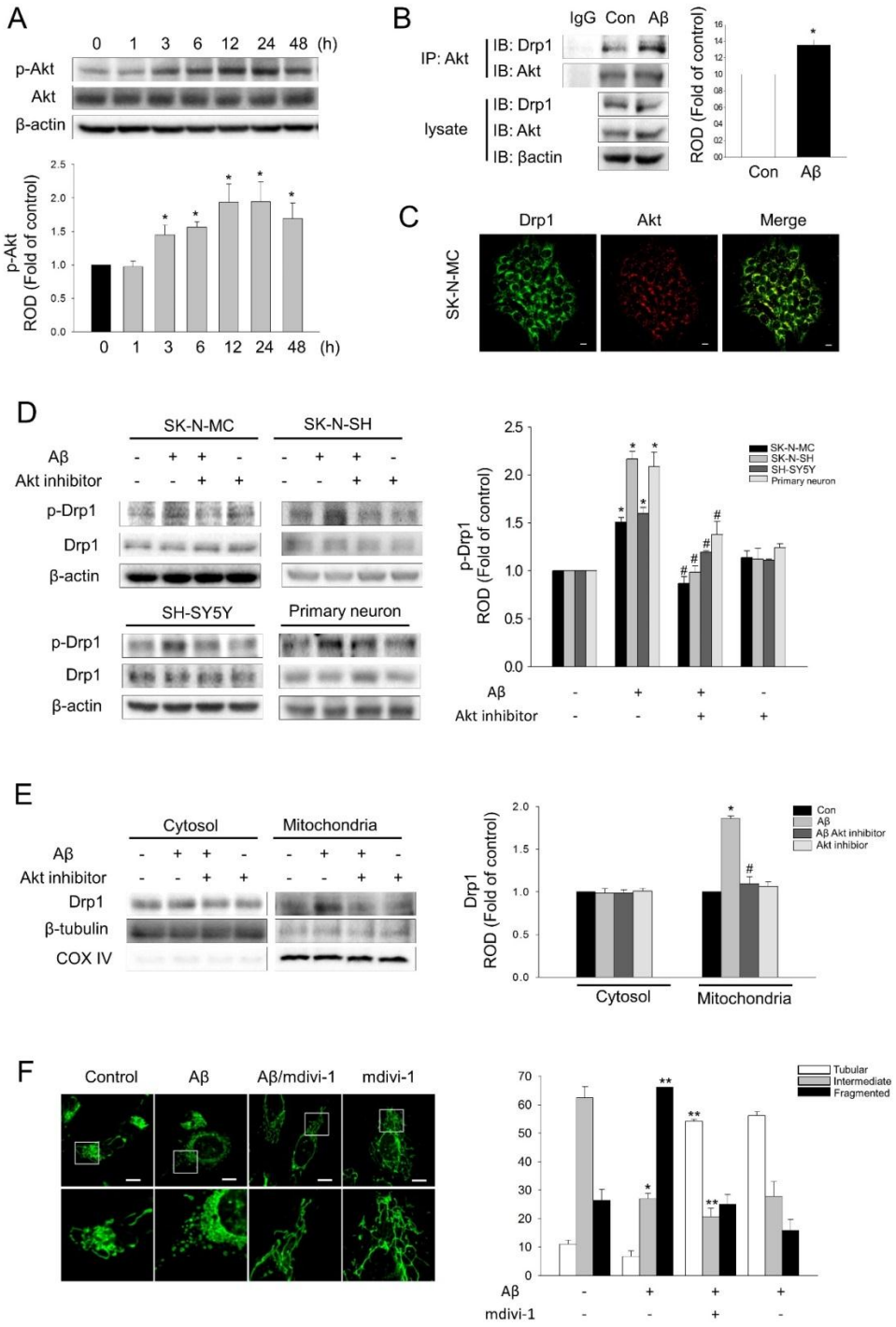
A
0 1 3 6 12 24 48 (h)
p-Akt
Akt
β-actin
p-Akt ROD (Fold of control)
B
IgG Con Aβ
IP: Akt
IB: Drp1
IB: Akt
lysate
IB: Drp1
IB: Akt
IB: βactin
ROD (Fold of control)
Con Aβ
C
Drp1 Akt Merge
SK-N-MC
D
SK-N-MC SK-N-SH
Aβ
Akt inhibitor
p-Drp1
Drp1
β-actin
SH-SY5Y Primary neuron
p-Drp1 ROD (Fold of control)
SK-N-MC
SK-N-SH
SH-SY5Y
Primary neuron
Aβ
Akt inhibitor
E
Cytosol Mitochondria
Aβ
Akt inhibitor
Drp1
β-tubulin
COX IV
Drp1 ROD (Fold of control)
Con
Aβ
Aβ Akt inhibitor
Akt inhibior
Cytosol
Mitochondria
F
Control Aβ Aβ/mdivi-1 mdivi-1
Tubular
Intermediate
Fragmented
Aβ
mdivi-1

Fig. 3 Aβ-induced sustained Akt activation regulates Drp1 phosphorylation. (A) SK-N-MC cells were treated with 5 μM Aβ for 0-48 h. Total cell lysates were subjected to western blotting, and phospho-AktSer473 and Akt expression levels were detected. The bars in the below panel denote mean ± SEM of three experiments for each condition determined by densitometry relative to total-Akt and to the loading control β-actin. *p<0.05 versus 0 h. (B) SK-N-MC cells were treated with Aβ (5 μM) for 6 h prior to harvesting. Akt protein was co-immunoprecipitated with Drp1. Cells were subjected to precipitation by Akt antibody. The precipitated complex was analyzed by western blotting and detected with Drp1 antibody (left). Expression of Drp1 and Akt in total cell lysates is shown (right). n=3, *p<0.05 versus control. IP: Immunoprecipitation, IB: Immunoblotting. (C) The colocalization of Drp1(green) with Akt(Red) was determined by confocal microscopy using immunofluorescence staining. Scale bar, 5 μM. n=3. (D) Three different neuronal cell lines and primary neurons were pretreated with/without Akt inhibitor (10 μM) for 30 min, and then exposed to Aβ (5 μM) for 48 h. The cell lysates were subjected to western blotting, and determined by phospho-Drp1Ser616 and Drp1 antibodies. The bars in the below part of panel denote mean ± SEM of three experiments for each condition determined by densitometry relative to total Drp1 and to the loading control β-actin. *p<0.05 versus control, #p<0.05 versus Aβ. (E) SK-N-MC cells were pretreated with/without Akt inhibitor (10 μM) for 30 min, and then exposed to Aβ (5 μM) for 48 h. Mitochondrial and Cytosolic fractions were mentioned in Materials and Methods. Anti-Drp1 antibody was used for western blotting. Anti-COX IV(mitochondria) and anti-β-tubulin(cytosol) was used as markers for each fraction. The bars in the below part of panel denote mean ± SEM

of three experiments for each condition determined by densitometry relative to total protein. *p<0.05 versus control, #p<0.05 versus Aβ. (F) SK-N-MC cells were pretreated with Mdivi-1 (1 μM) and then exposed to Aβ (5 μM) for 48h and then loaded with MitoTracker Green (200 nM). Representative images were obtained by confocal microscopy. The individual mitochondrial length was assessed and classified into three different categories and quantified as percentage. Data represent mean ± SEM of ten random fields from three experiments for each condition. Scale bar, 5 μm. *p<0.05 versus control, **p<0.01 versus control.

3. The role of ROS in Aβ-induced mitochondrial dysfunction

To determine whether excessive mitochondrial fission by Aβ stimulation affects its abilities, I assessed the function of mitochondria. The levels of ROS increased with time and significantly increased at 6 hours up to 140% (Figure 4A). The Aβ-induced ROS generation was attenuated by pretreatment with Mito-Tempo and NAC, suggesting that mitochondria, as a major source of ROS, was induced by Aβ (Figure 4B). Furthermore, inhibition of mitochondrial fission by Mdivi-1 decreased the Aβ-induced ROS levels showing that mitochondrial fission has a critical role in ROS generation (Figure 4C). In addition, Aβ decreased the mitochondrial membrane potential ($\Delta\Psi$m) which was confirmed by JC-1 staining. Green fluorescence increased when treated with Aβ, indicating the loss of $\Delta\Psi$m. Pretreatment with Mdivi-1 and Aβ showed a great increase in red fluorescence, suggesting the recovery of $\Delta\Psi$m. Concurrently, Aβ-induced $\Delta\Psi$m disruption was prevented by pretreatment with NAC, indicating that ROS generation by Aβ precede depolarization

of $\Delta\Psi$m (Figure 5A). Aβ started to increase the level of cellular ATP at 24 hours but was significantly decreased at 48 hours down to 40% (Figure 5B). Interestingly, I found a significant correlation between the morphological changes in mitochondria and the total ATP levels. Exposure to Aβ for 24 h resulted in elongated mitochondria while becoming fragmented at 48 h. Moreover, Aβ-induced ATP depletion was prevented by Mdivi-1 and also Akt inhibitor pretreatment as expected (Figure 5C). Therefore, my results show that mitochondrial morphology played a critical role in maintaining the function of mitochondria and that Aβ induced mitochondria fission resulting in mitochondrial dysfunction.

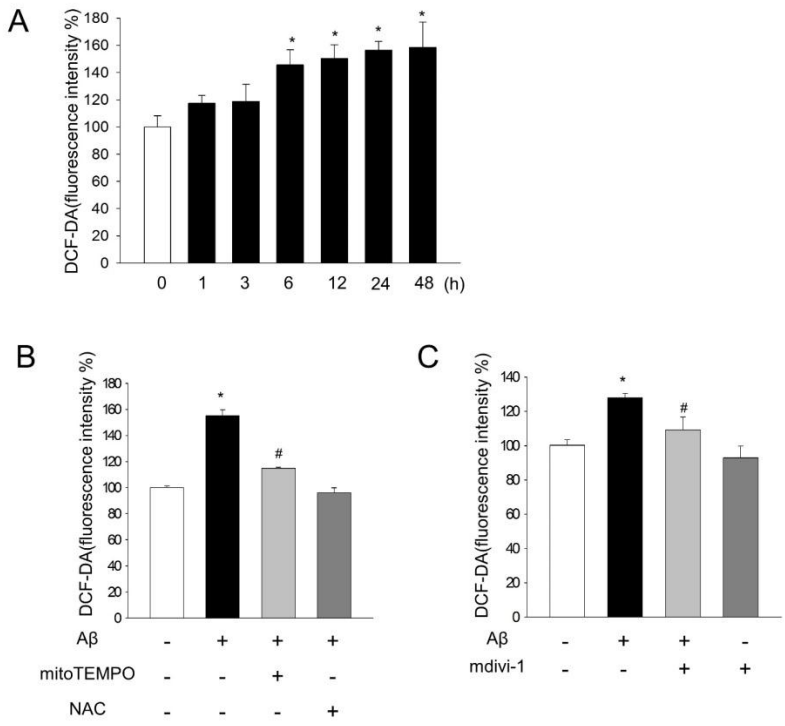

Fig. 4 Aβ impairs mitochondrial function through mitochondrial fission. (A) After SK-N-MC was treated with Aβ (5 μM) in a time-dependent manner, H2DCF-DA was incubated for 30 min to detect ROS and it was measured by using luminometer. n=5. *p<0.05 versus 0 h. (B) The SK-N-MC cells were pretreated with mitoTEMPO (1 μM) and NAC (5 mM) for 30 min and incubated with Aβ (5 μM) for 48 hours. Then H2DCF-DA was incubated for 1 hour to detect ROS and it was measured by using luminometer. The bars in the below part of panel denote mean ± SEM of five experiments for each condition. *p<0.05 versus control, #p<0.05 versus Aβ. (C) The SK-N-MC cells were pretreated with mdivi-1 (1 μM) for 30 min and incubated with Aβ (5 μM) for 48 hours. Then H2DCF-DA was

incubated for 1 hour to detect ROS and it was measured by using luminometer. The bars in the below part of panel denote mean ± SEM of three experiments for each condition. *p<0.05 versus control, #p<0.05 versus Aβ.

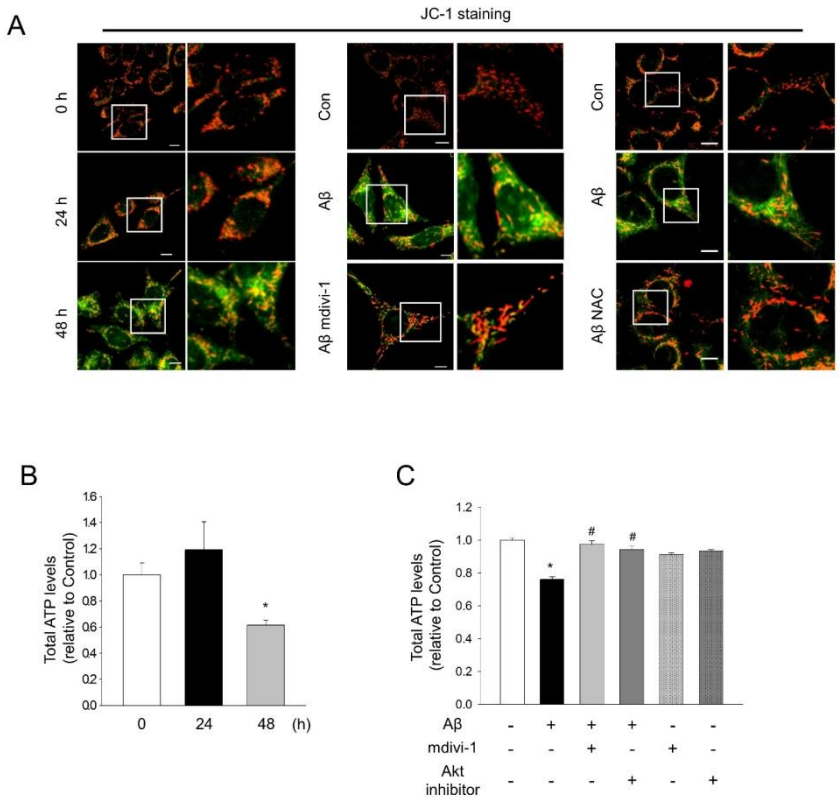

Fig. 5 Assessment of mitochondrial function affected by Aβ. (A) SK-N-MC cells were pretreated with mdivi-1 (1 μM) and NAC (5 mM) for 30min, and then exposed to Aβ (5 μM) for 48h. Cells were stained with JC-1, and mitochondrial membrane potential was measured by confocal. Representative images were obtained from three experiments for each condition. Scale bar, 5 μm. (B) SK-N-MC cells were treated with Aβ (5 μM) for 0-48h. Intracellular ATP level was measured and then normalized to cellular protein. Data represent mean ± SEM. n=5. *p<0.05 versus control. (C) SK-N-MC cells were pretreated with mdivi-1 (1 μM)

and Akt inhibitor (10 μM) for 30 min, and then exposed to Aβ (5 μM) for 48h. Intracellular ATP level was measured and then normalized to cellular protein. Data represent mean ± SEM. n=5. *p<0.05 versus control, #p<0.05 versus Aβ.

4. Inhibition of autophagy through Akt/mTOR signaling leads to neuronal apoptosis.

To further show the pivotal role of Akt phosphorylation, I investigated whether there is any link between Akt activation and autophagy inhibition in Aβ-induced mitochondrial dysfunction. Aβ enhanced the phosphorylation level of mTOR was reversed by an Akt inhibitor (Figure 6A). Aβ-induced mTOR activation inhibited the rate of LC3-I to LC3-II conversion which was increased with Rapamycin (an mTOR inhibitor) (Figure 6B). Next, Rapamycin and Trehalose (mTOR dependent/ independent autophagy enhancers) were used to clarify whether autophagic failure by Aβ could prevent mitochondrial dysfunction. As expected, not only Rapamycin but also Trehalose decreased the level of Aβ-induced ROS generation indicating that the decreased autophagy clearance accelerated mitochondrial dysfunction (Figure 6C). Furthermore, the inhibition of autophagy with 3-MA (autophagy inhibitor) showed activation of caspase 9 and 3, suggesting that impairment of autophagy leads to functional problems of mitochondria (Figure 6D).

To investigate how mitochondrial ROS aggravated by impaired autophagic clearance could lead to neuronal apoptosis, I examined the molecular markers of apoptosis induced by Aβ. A significant release of cytochrome C was observed from mitochondria to cytosol, which was inhibited by Mdivi-1 (Figure 7A). Aβ significantly increased Bax/Bcl-2 ratio, in particular, an increase in Bax expression was observed while Bcl-2 expression had no significant change in human neuronal cell lines (Figure 8A). Release of Cytochrome C by Aβ induced the activation of caspases. Aβ treatment increased the cleavage of caspase 9 and 3 with time, which was also blocked by NAC (Figure 8B and 8C). Consistently, the trypan blue assay showed that the rate of Aβ-induced apoptotic cells (44%) was reversed by NAC pretreatment (15%) (Figure 8D). Furthermore, Aβ increased apoptosis at the late stages (20.95±2.43%) compared with the control (10±0.69%). In contrast, NAC showed a significant decrease in the apoptosis rate, supporting that Aβ-induced dysfunction of mitochondria accelerated neuronal apoptosis (Figure 8E). Taken together, my data confirm that Akt-induced autophagic inhibition elevates mitochondrial ROS which plays a crucial role in exacerbating neuronal apoptosis through the accumulation of damaged

mitochondria.

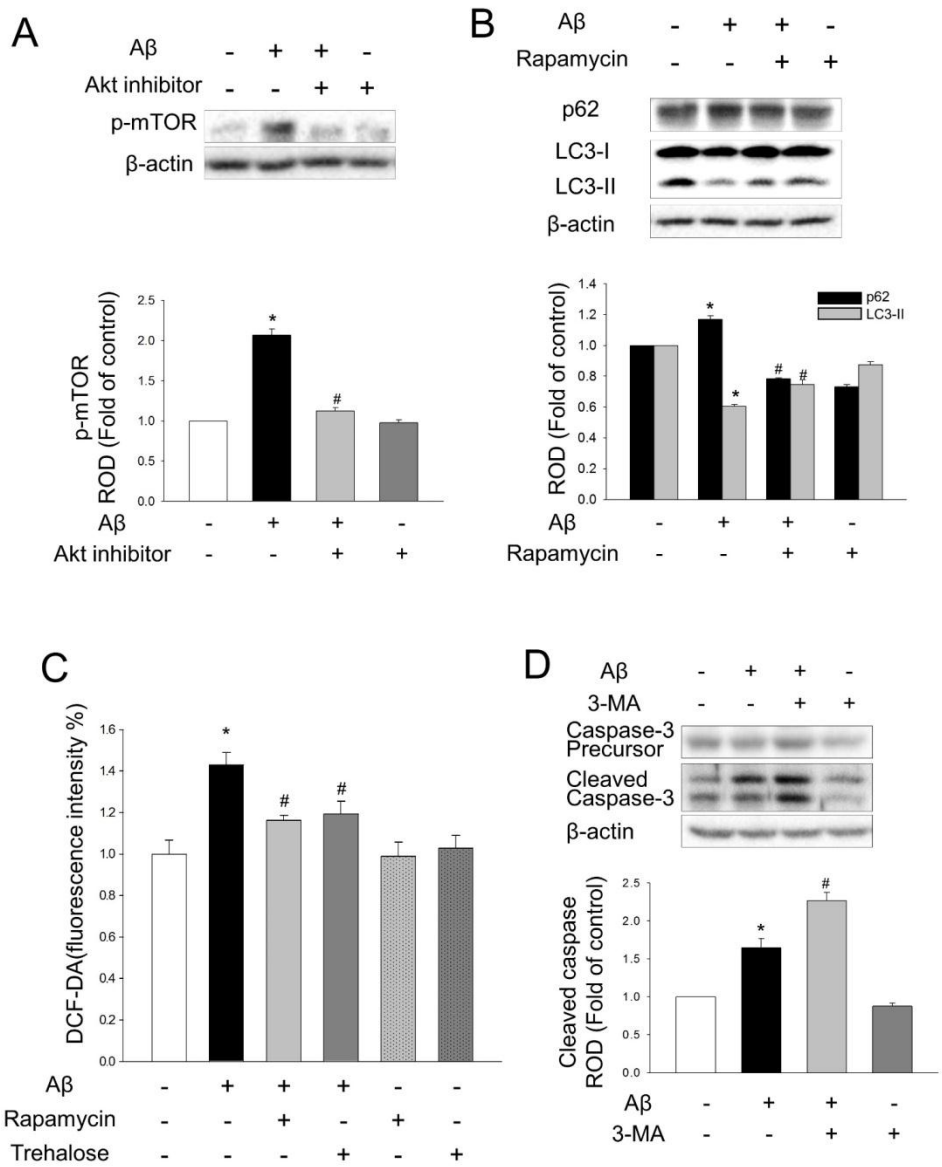

Fig. 6 Inhibition of autophagy by Aβ leads to abnormal mitochondrial accumulation. (A) SK-N-MC pretreated with/without Akt inhibitor (10 μM) for 30 min, and then exposed to Aβ (5 μM) for 48 h. The cell lysates were subjected to western

blotting, and determined by phospho-mTORSer2448 antibody. The bars in the below part of panel denote mean ± SEM of three experiments for each condition determined by densitometry relative to the loading control β-actin. *p<0.05 versus control, #p<0.05 versus Aβ. (B) SK-N-MC pretreated with/without Rapamycin (10 nM) for 30 min, and then exposed to Aβ (5 μM) for 48 h. The cell lysates were subjected to western blotting, and determined by p62 and LC3 antibodies. The bars in the below part of panel denote mean ± SEM of three experiments for each condition determined by densitometry relative to β-actin. *p<0.05 versus control, #p<0.05 versus Aβ. (C) The SK-N-MC was pretreated with Rapamycin (10 nM) and Trehalose (10 μM) for 30 min and it was incubated with Aβ (5 μM) for 48 hours. Then H2DCF-DA was incubated for 1 hour to detect ROS and it was measured by using luminometer. The bars in the below part of panel denote mean ± SEM of three experiments for each condition. *p<0.05 versus control, #p<0.05 versus Aβ. (D) SK-N-MC cells were pretreated with/without 3-MA (10 μM) for 30 min, and then exposed to Aβ (5 μM) for 48 h, The total cell lysates were subjected to western blotting and caspase-9 and caspase-3 levels were detected. The bars in the below part of panel denote mean ± SEM of three experiments for each condition determined by densitometry relative to total protein. *p<0.05 versus control, #p<0.05 versus Aβ.

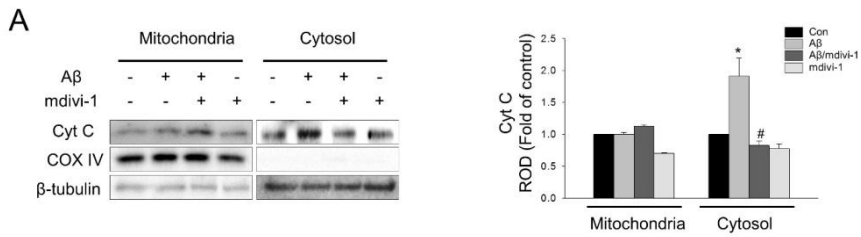

Fig. 7 Inhibition of mitochondrial fission attenuates cytochrome C release. (A) SK-N-MC cells were pretreated with/without mdivi-1 (1 μM) for 30 min, and then exposed to Aβ (5 μM) for 48 h. Mitochondrial and Cytosolic fractions were mentioned in *Materials and Methods*. Anti-cytochrome C antibody was used for western blotting. Anti-COX IV(mitochondria) and anti-β-tubulin(cytosol) was used as markers for each fraction. The bars in the below part of panel denote mean ± SEM of three experiments for each condition determined by densitometry relative to total protein. *p<0.05 versus control, #p<0.05 versus Aβ.

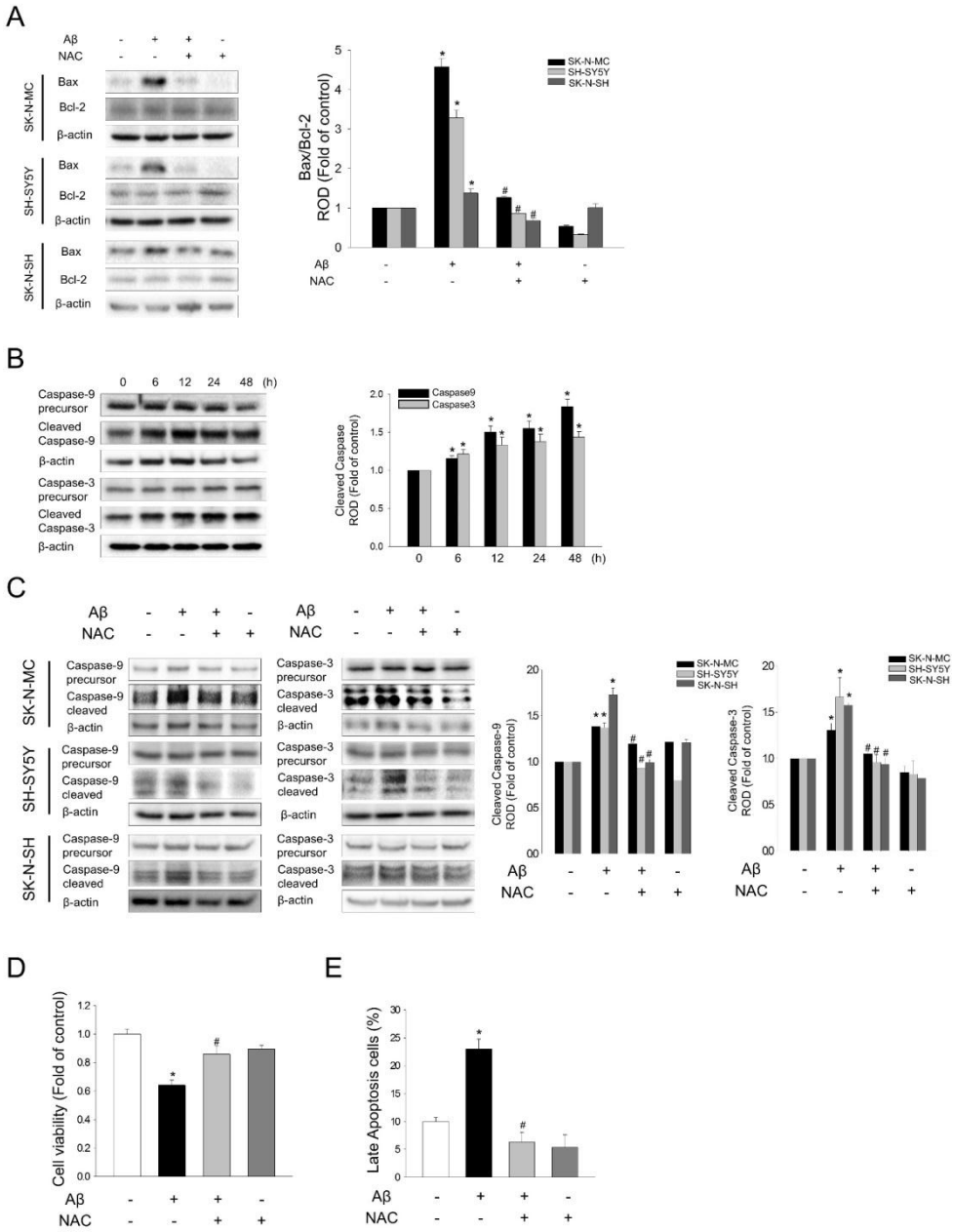

Fig. 8 Aβ−induced mitochondrial dysfunction lead to neuronal apoptosis. (A) Three different neuronal cell lines were pretreated with/without NAC (5 mM) for 30 min, and then exposed to Aβ (5 μM) for 48 h. The cell lysates were subjected to

western blotting, and determined by Bax and Bcl-2 antibodies. The bars in the below part of panel denote mean ± SEM of three experiments for each condition determined by densitometry relative to total protein. *p<0.05 versus control, #p<0.05 versus Aβ. (B) SK-N-MC cells were treated with 5 μM Aβ for 0-48 h. Total cell lysates were subjected to western blotting, and caspase-9 and caspase-3 were detected. The bars in the below panel denote mean ± SEM of three experiments for each condition determined by densitometry relative to β-actin *p<0.05 versus 0 h. (C) Three different neuronal cell lines were pretreated with/without NAC (5 mM) for 30 min, and then exposed to Aβ (5 μM) for 48 h. The cell lysates were subjected to western blotting, and determined by pro-caspase-9, cleaved caspase-9, pro-caspase-3 and cleaved caspase-3 antibodies. The bars in the below part of panel denote mean ± SEM of three experiments for each condition determined by densitometry relative to total protein. *p<0.05 versus control, #p<0.05 versus Aβ. (D) SK-N-MC was pretreated with/without NAC (5 mM) for 30 min, and then exposed to Aβ (5 μM) for 48 h. Cell viability were measured by Trypan blue exclusion assay mentioned in Materials and Methods. Data represent mean ± SEM. n=5. *p<0.05 versus control, #p<0.05 versus Aβ. (E) Quantitative analysis of the fold changes of late apoptotic cells were measured by using annexin V/proidium iodide (PI) staining. SK-N-MC cells were pretreated with/without NAC (5 mM) and then, exposed to Aβ. The cells were stained with Annexin V (25 μg/ml) and PI (125 ng/ml), and incubated for 30min at room temperature in the dark and quantified by FACs. Data represent mean ± SEM. n=5. *p<0.05 versus control, #p<0.05 versus Aβ.

DISCUSSION

Alteration of mitochondrial dynamic proteins and excessive fragmentation of mitochondria in the AD brain suggest the close association between mitochondrial dynamics and AD pathogenesis [16] [17] [18]. The current study showed that Aβ phosphorylated the Drp1 through Akt signaling, leading to mitochondrial fission-mediated neuronal apoptosis (Figure 9). Previous works showed that mitochondrial fusion and fission were modulated in stress-induced circumstances. In the mild stress circumstances, mitochondria fused together as a compensatory response by exchanging their compartments [19]. A unified network of mitochondria gave the impaired mitochondria a chance to survive by mixing their contents. Meanwhile, disruption of the mitochondrial network by severe stress induced the excessive mitochondria fragmentation and dysfunction, leading to apoptosis [20]. These findings were consistent with my results in which low levels of Aβ showed the interconnected form of high concentrations with long exposure of Aβ, resulted in the fragmentation of mitochondria in SK-N-MC cells. Accumulating

evidences suggested that Aβ induced neuronal apoptosis through mitochondrial fragmentation thereby leading to Alzheimer's diseases [21] [22]. I substantiated this evidence by showing that Aβ-induced neuronal apoptosis was prevented by inhibition of mitochondrial fragmentation not only in neuronal cell lines but also in primary neurons. These findings indicate that regulation of the mitochondrial dynamics can be a therapeutic target for AD.

The present work showed that there were no significant changes in the levels of proteins and mRNAs expression which were involved in the mitochondrial fission/fusion regulators (Figure 10A and 10B). My work suggested strongly that there would be another way for the regulation of the dynamic protein activities. Drp1 phosphorylation is well known to be the most common form of post-translational modification. There are two major sites of phosphorylation in Drp1, namely Ser 616 and Ser 637, which induce and inhibit the translocation of mitochondria, respectively [23]. My work showed that the phosphorylation of Drp1 Ser 616 translocated to the outer membrane in the mitochondria and assembled with itself. The ring-like oligomerization of Drp1 facilitated the activities of GTP, leading to the constriction and fragmentation of mitochondria [24]. Thus,

upstream signals would control the Drp1 translocation from the cytosol to mitochondria, and these play an important role in the fission of mitochondria, which regulates the neuronal cell fate.

Since that less is known about the modulator, which regulates mitochondrial fission and fusion proteins, consequently, cellular physiological circumstances undergoing mitochondrial fission have been studied. Akt is known to serve as key regulating molecules of cell survival and proliferation [25]. However, Akt activation did not always show the positive effect in relation to the cell survival. A recent study showed that aberrant Akt activation leads to the deleterious effects such as NFT formation in the AD brain and contributes to the severity of the AD pathogenesis [26]. Other studies also demonstrated that over-activation of Akt has been observed in the progression of AD brain [27] [28]. Accumulating evidences imply that Akt acts as a death kinase through regulating the balance of apoptosis and survival. In consistency with the previous works, my results showed that Akt activation induced by A β was maintained up to 48 h and sustained but not transient. This prompted us to examine the Akt signaling as a dominant regulator in AD. Little is known about the exact machinery of sustained Akt,

which has a double edged sword in neuronal cell death. Multiple pathways were recently suggested for maintaining the Akt activation which is responsible for the programmed cell death [29]. Thus, early event in Aβ-altered signals regulating the phosphorylation of Akt such as uncontrolled calcium influx was investigated. My work showed that Aβ increased the bulk of calcium entry through the N-methyl-D-aspartatenreceptor (NMDAR) and L-type voltage-gated calcium channel (L-VGCC). Additionally, Aβ-induced intracellular calcium overload activated the downstream molecule of calcium-dependent signaling, and increased the level of CaMKII phosphorylation. CaMKII is known to phosphorylate the various signal molecules involved in memory formation and neuronal functions [30]. In normal status, CaMKII phosphorylation of Thr286 lasts for a short time to neuronal survival. However, it also promotes the neuronal cell death through prolonged activation. Dysregulation of phosphorylation in CaMKII is known to be deeply involved in AD pathogenesis [31]. Even though the precise machinery of the sustained activation of CaMKII is not completely understood, however, it could be speculated from my results that Aβ extended the activation of CaMKII through a large amount of calcium influx,

which directly mediates the sustained-phosphorylation of Akt.

Akt, once phosphorylated, is rapidly translocated to the numerous subcellular organelles [32]. However, the interaction between Akt and Drp1 as one of the key molecules regulating mitochondrial fission has not been much studied so far. My work showed, as expected, that pretreatment with Akt inhibitor remarkably decreased the levels of Drp1 phosphorylation and prevented the Drp1 translocation to mitochondria. This suggests that Drp1 is a novel direct substrate of Akt. My results also indicated that the Drp1 activity was regulated by sustaining the Akt through its direct binding to Akt. This Akt-Drp1 interaction induced the Drp1 phosphorylation and lead to the mitochondrial fission. Inhibition of mitochondrial fission through Mdivi-1 was investigated to examine whether Aβ-induced massive fragmentation of mitochondria promoted their dysfunction. Recently correlation between mitochondrial fission and cytochrome C release during apoptosis was found and the leakage of mitochondrial intermembrane space (IMS) contents was promoted [33]. Drp1, the mitochondrial fission protein, promoted the release of cytochrome C was also observed [34] [35]. In accordance with those works, my work also showed that the release of cytochrome C was attenuated

by inhibiting mitochondrial fission and that mitochondrial ROS was triggered by leakage of cytochrome C during mitochondrial fission. Further studies are needed to better understand of precise machinery on the increase of ROS by mitochondrial fragmentation.

Mitochondrial electronic transport is well known as the major source of ROS and that neuronal death was caused by ROS [36]. My work showed that massive ROS generation was accompanied by $\Delta\Psi$m collapse and ATP loss in response to Aβ. Once Aβ increased the intracellular ROS levels, prolonged oxidative stress provoked the mitochondrial alterations (e.g., $\Delta\Psi$m disruption and ATP depletion). My work also showed that the production of ROS induced by Aβ resulted in the loss of mitochondrial potential. All of these $\Delta\Psi$m collapses were attenuated by both mdivi1 and NAC, suggesting that ROS generation preceded the $\Delta\Psi$m dissipation. Aβ−induced loss of mitochondrial membrane potential leads to the low efficiency of the proton motive force causing ATP depletion. Aβ−induced alteration of total ATP was observed between 24 and 48 h, suggesting that mitochondrial morphology is responsible for producing ATP. It can be speculated that the increase of total ATP levels at 24 hours would be compensated through mitochondrial elongation, maintaining the

ATP levels. In addition, inhibition of oxidative stress prevented the $\Delta\Psi$m disruption and the ATP depletion, indicating that mitochondrial ROS was the direct cause of their dysfunction. Furthermore, my work showed that ROS induced not just the mitochondrial dysfunction but also the activation of caspase, which lead to neuronal apoptosis. Thus, my work suggested strongly that management of intracellular ROS mediated by mitochondrial fission would be a potent therapeutic target in neuronal apoptosis.

Another role of the sustained activation of Akt/ mTOR is the autophagic dysfunction [37]. Impairment of autophagy induces the aggregation of misfolded proteins and organelles through an aberrant Akt/ mTOR pathway in AD pathogenesis [38]. Excessive mitochondria fragmentation has been reported to promote mitochondrial autophagy [39] [40]. Mitochondrial fission proteins, such as Drp1, act as adaptor protein in direct combination with LC3-II phagophore membranes and lead to mitochondrial autophagy [41]. However, my work exhibited that Aβ-induced mitochondrial fission did not increase the level of autophagy. In contrast, the level of autophagy markers was decreased by Aβ. Inhibition of autophagy even by mitochondrial fragmentation prompted us to think about other

possibility that impairs autophagy. It has been accepted that mitochondrial fission in general triggered the possibility of autophagy. However, my work suggests that mitochondrial fragmentation is not always sufficient to induce mitochondrial autophagy. It can be speculated that Aβ would disrupt the initiation stage of autophagic machinery through mTOR activation. In another words, conjugation cascade of autophagy by mitochondrial fragmentation could not proceed without vesicle nucleation. The abnormal mitochondria would be accumulated by inhibited autophagy, which amplify the mitochondrial dysfunction and result in neuronal apoptosis. It should be noted that up-regulation of autophagy partially prevented Aβ toxicity in neuronal cells by attenuating mitochondrial dysfunction such as ROS generation [42]. It is obvious that Akt/mTOR signaling or interacting mechanism between Akt/mTOR and Drp1 have a crucial effect on the development and progression of AD pathology. Thus, basic research is necessary to further clarify their roles as a potential therapeutic target in AD.

In conclusion, Aβ-induced Akt phosphorylation directly activated the Drp1 leading excessive mitochondrial fragmentation. Also, autophagy impairment through Akt/mTOR signaling accumulates

abnormal mitochondria, which cause ROS mediated neuronal apoptosis.

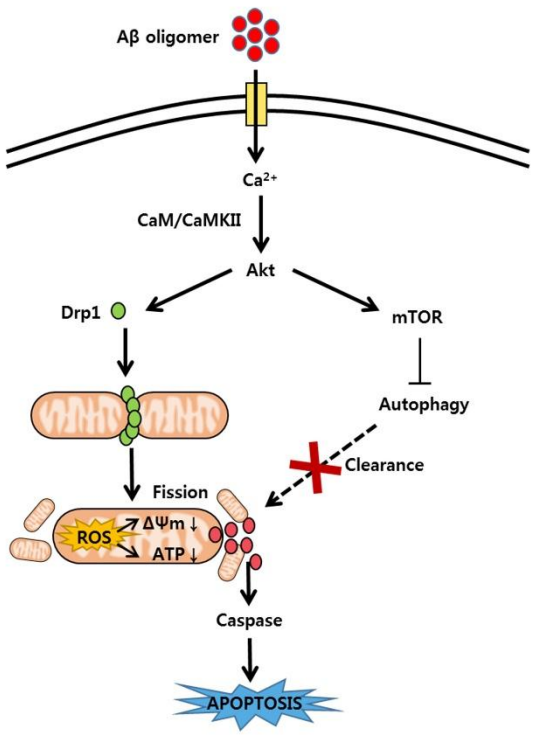

Fig. 9 Aβ-Induced mitochondrial fission mediated neuronal apoptosis. A proposed scheme about the effect of Aβ in mitochondrial fragmentations resulting in neuronal apoptosis.

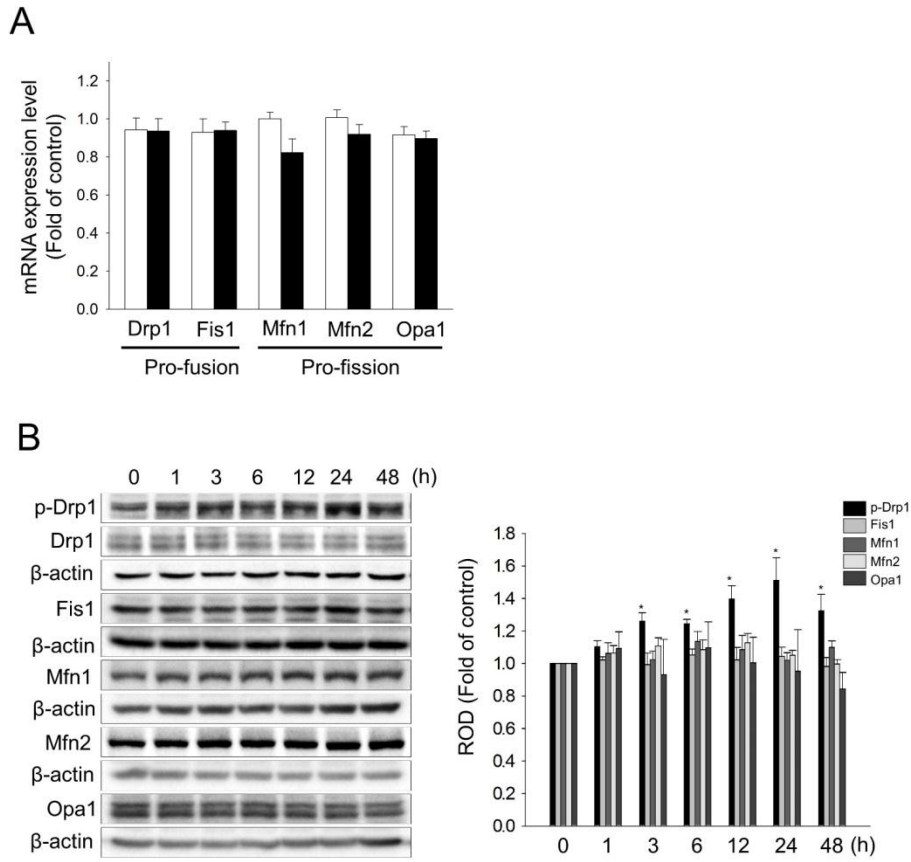

Fig. 10 The alteration of mitochondrial dynamics proteins and mRNAs expression levels by Aβ. (A) SK-N-MC cells were treated with Aβ (5 μM) for 48h and then extracted the RNA. Mitochondrial dynamics proteins were determined with real-time PCR. The bars represent mean ± SEM of three experiments for each condition. *p<0.05 versus control. (B) SK-N-MC cells were treated with 5 μM Aβ for 0-48 h. Total cell lysates were subjected to western blotting, and Mfn1/2, Opa1, Fis1, phospho-Drp1 and Drp1 levels were detected. The bars in the below panel denote mean ± SEM of three experiments for each condition determined by densitometry relative to the loading control β-actin. *p<0.05 versus 0 h.

Species	Genes	Accession Number	Sense	Antisense
Human	Drp1	BC024590	5’ -CAGTGTGCCAAAGGCAGTAA-3’	5’ -GATGAGTCTCCCGGATTTCA-3’
	Fis1	NM_016068	5’ -CTTGCTGTGTCCAAGTCCAA-3’	5’ -GCTGAAGGACGAATCTCAGG-3’
	Mfn1	NM_033540	5’ -TGTTTTGGTCGCAAACTCTG-3’	5’ -CTGTCTGCGTACGTCTTCCA-3'
	Mfn2	BC024590	5’ -TGTTGGCTCAGTGCTTCATC-3’	5’ -AAGTCCCTCCTTGTCCCAGT-3’
	Opa1	BC75805	5’ -GCAATGGGATGCAGCTATTT-3’	5’ -GCAAGATAAGCTGGGTGCTC-3’

Table 1. Primer sequences for RT-PCR amplification

References

[1] R.A. Marr, D.M. Hafez, Amyloid−beta and Alzheimer's disease: the role of neprilysin−2 in amyloid−beta clearance, Frontiers in aging neuroscience, 6 (2014) 187.

[2] D.F. Silva, A.R. Esteves, C.R. Oliveira, S.M. Cardoso, Mitochondria: the common upstream driver of amyloid−beta and tau pathology in Alzheimer's disease, Current Alzheimer research, 8 (2011) 563−572.

[3] W.L. Klein, Synaptotoxic amyloid−beta oligomers: a molecular basis for the cause, diagnosis, and treatment of Alzheimer's disease?, Journal of Alzheimer's disease : JAD, 33 Suppl 1 (2013) S49−65.

[4] M. Verri, O. Pastoris, M. Dossena, R. Aquilani, F. Guerriero, G. Cuzzoni, L. Venturini, G. Ricevuti, A.I. Bongiorno, Mitochondrial alterations, oxidative stress and neuroinflammation in Alzheimer's disease, International journal of immunopathology and pharmacology, 25 (2012) 345−353.

[5] P.I. Moreira, C. Carvalho, X. Zhu, M.A. Smith, G. Perry, Mitochondrial dysfunction is a trigger of Alzheimer's disease

pathophysiology, Biochimica et biophysica acta, 1802 (2010) 2-10.

[6] H.B. Suliman, C.A. Piantadosi, Mitochondrial Quality Control as a Therapeutic Target, Pharmacol Rev, 68 (2016) 20-48.

[7] G.P. Eckert, K. Renner, S.H. Eckert, J. Eckmann, S. Hagl, R.M. Abdel-Kader, C. Kurz, K. Leuner, W.E. Muller, Mitochondrial dysfunction--a pharmacological target in Alzheimer's disease, Molecular neurobiology, 46 (2012) 136-150.

[8] B. DuBoff, M. Feany, J. Gotz, Why size matters - balancing mitochondrial dynamics in Alzheimer's disease, Trends in neurosciences, 36 (2013) 325-335.

[9] P.H. Reddy, R. Tripathi, Q. Troung, K. Tirumala, T.P. Reddy, V. Anekonda, U.P. Shirendeb, M.J. Calkins, A.P. Reddy, P. Mao, M. Manczak, Abnormal mitochondrial dynamics and synaptic degeneration as early events in Alzheimer's disease: implications to mitochondria-targeted antioxidant therapeutics, Biochimica et biophysica acta, 1822 (2012) 639-649.

[10] A.Y. Seo, A.M. Joseph, D. Dutta, J.C. Hwang, J.P. Aris, C. Leeuwenburgh, New insights into the role of mitochondria in aging: mitochondrial dynamics and more, Journal of cell science, 123 (2010) 2533-2542.

[11] C.S. Palmer, L.D. Osellame, D. Stojanovski, M.T. Ryan, The regulation of mitochondrial morphology: intricate mechanisms and dynamic machinery, Cellular signalling, 23 (2011) 1534-1545.

[12] X.J. Han, K. Tomizawa, A. Fujimura, I. Ohmori, T. Nishiki, M. Matsushita, H. Matsui, Regulation of mitochondrial dynamics and neurodegenerative diseases, Acta medica Okayama, 65 (2011) 1-10.

[13] B. Cho, S.Y. Choi, H.M. Cho, H.J. Kim, W. Sun, Physiological and pathological significance of dynamin-related protein 1 (drp1)-dependent mitochondrial fission in the nervous system, Experimental neurobiology, 22 (2013) 149-157.

[14] J. Park, H. Choi, J.S. Min, B. Kim, S.R. Lee, J.W. Yun, M.S. Choi, K.T. Chang, D.S. Lee, Loss of mitofusin 2 links beta-amyloid-mediated mitochondrial fragmentation and Cdk5-induced oxidative stress in neuron cells, Journal of neurochemistry, 132 (2015) 687-702.

[15] A. Jahani-Asl, E. Huang, I. Irrcher, J. Rashidian, N. Ishihara, D.C. Lagace, R.S. Slack, D.S. Park, CDK5 phosphorylates DRP1 and drives mitochondrial defects in NMDA-induced neuronal death, Human molecular genetics, 24 (2015) 4573-4583.

[16] F. Burte, V. Carelli, P.F. Chinnery, P. Yu-Wai-Man, Disturbed

mitochondrial dynamics and neurodegenerative disorders, Nature reviews. Neurology, 11 (2015) 11-24.

[17] M.J. Calkins, M. Manczak, P. Mao, U. Shirendeb, P.H. Reddy, Impaired mitochondrial biogenesis, defective axonal transport of mitochondria, abnormal mitochondrial dynamics and synaptic degeneration in a mouse model of Alzheimer's disease, Human molecular genetics, 20 (2011) 4515-4529.

[18] M. Manczak, M.J. Calkins, P.H. Reddy, Impaired mitochondrial dynamics and abnormal interaction of amyloid beta with mitochondrial protein Drp1 in neurons from patients with Alzheimer's disease: implications for neuronal damage, Human molecular genetics, 20 (2011) 2495-2509.

[19] C. Blackstone, C.R. Chang, Mitochondria unite to survive, Nature cell biology, 13 (2011) 521-522.

[20] H. Otera, N. Ishihara, K. Mihara, New insights into the function and regulation of mitochondrial fission, Biochimica et biophysica acta, 1833 (2013) 1256-1268.

[21] P. Picone, D. Nuzzo, L. Caruana, V. Scafidi, M. Di Carlo, Mitochondrial dysfunction: different routes to Alzheimer's disease therapy, Oxidative medicine and cellular longevity, 2014 (2014)

780179.

[22] R.J. Youle, M. Karbowski, Mitochondrial fission in apoptosis, Nature reviews. Molecular cell biology, 6 (2005) 657-663.

[23] H. Otera, K. Mihara, Mitochondrial dynamics: functional link with apoptosis, International journal of cell biology, 2012 (2012) 821676.

[24] R.W. Clinton, C.A. Francy, R. Ramachandran, X. Qi, J.A. Mears, Dynamin-related Protein 1 Oligomerization in Solution Impairs Functional Interactions with Membrane-anchored Mitochondrial Fission Factor, The Journal of biological chemistry, 291 (2016) 478-492.

[25] G. Song, G. Ouyang, S. Bao, The activation of Akt/PKB signaling pathway and cell survival, Journal of cellular and molecular medicine, 9 (2005) 59-71.

[26] Y. Kitagishi, A. Nakanishi, Y. Ogura, S. Matsuda, Dietary regulation of PI3K/AKT/GSK-3beta pathway in Alzheimer's disease, Alzheimer's research & therapy, 6 (2014) 35.

[27] O.N. C, PI3-kinase/Akt/mTOR signaling: impaired on/off switches in aging, cognitive decline and Alzheimer's disease, Experimental gerontology, 48 (2013) 647-653.

[28] A. Tramutola, J.C. Triplett, F. Di Domenico, D.M. Niedowicz,

M.P. Murphy, R. Coccia, M. Perluigi, D.A. Butterfield, Alteration of mTOR signaling occurs early in the progression of Alzheimer disease (AD): analysis of brain from subjects with pre-clinical AD, amnestic mild cognitive impairment and late-stage AD, Journal of neurochemistry, 133 (2015) 739-749.

[29] Q. Liu, J. Qiu, M. Liang, J. Golinski, K. van Leyen, J.E. Jung, Z. You, E.H. Lo, A. Degterev, M.J. Whalen, Akt and mTOR mediate programmed necrosis in neurons, Cell death & disease, 5 (2014) e1084.

[30] M. Stratton, I.H. Lee, M. Bhattacharyya, S.M. Christensen, L.H. Chao, H. Schulman, J.T. Groves, J. Kuriyan, Activation-triggered subunit exchange between CaMKII holoenzymes facilitates the spread of kinase activity, eLife, 3 (2014) e01610.

[31] A. Ghosh, K.P. Giese, Calcium/calmodulin-dependent kinase II and Alzheimer's disease, Molecular brain, 8 (2015) 78.

[32] D. Min, F. Guo, S. Zhu, X. Xu, X. Mao, Y. Cao, X. Lv, Q. Gao, L. Wang, T. Chen, C. Shaw, L. Hao, J. Cai, The alterations of Ca2+/calmodulin/CaMKII/CaV1.2 signaling in experimental models of Alzheimer's disease and vascular dementia, Neuroscience letters, 538 (2013) 60-65.

[33] C.D. Fan, M.A. Lum, C. Xu, J.D. Black, X. Wang, Ubiquitin-dependent regulation of phospho-AKT dynamics by the ubiquitin E3 ligase, NEDD4-1, in the insulin-like growth factor-1 response, The Journal of biological chemistry, 288 (2013) 1674-1684.

[34] R. Ban-Ishihara, T. Ishihara, N. Sasaki, K. Mihara, N. Ishihara, Dynamics of nucleoid structure regulated by mitochondrial fission contributes to cristae reformation and release of cytochrome c, Proceedings of the National Academy of Sciences of the United States of America, 110 (2013) 11863-11868.

[35] J. Estaquier, D. Arnoult, Inhibiting Drp1-mediated mitochondrial fission selectively prevents the release of cytochrome c during apoptosis, Cell death and differentiation, 14 (2007) 1086-1094.

[36] E. Holzerova, H. Prokisch, Mitochondria: Much ado about nothing? How dangerous is reactive oxygen species production?, The international journal of biochemistry & cell biology, 63 (2015) 16-20.

[37] Y. Hua, Y. Zhang, A.F. Ceylan-Isik, L.E. Wold, J.M. Nunn, J. Ren, Chronic Akt activation accentuates aging-induced cardiac hypertrophy and myocardial contractile dysfunction: role of

autophagy, Basic research in cardiology, 106 (2011) 1173-1191.

[38] O.V. Akopova, L.I. Kolchinskaya, V.I. Nosar, V.A. Bouryi, I.N. Mankovska, V.F. Sagach, Cytochrome C as an amplifier of ROS release in mitochondria, Fiziolohichnyi zhurnal (Kiev, Ukraine : 1994), 58 (2012) 3-12.

[39] W. Zuo, S. Zhang, C.Y. Xia, X.F. Guo, W.B. He, N.H. Chen, Mitochondria autophagy is induced after hypoxic/ischemic stress in a Drp1 dependent manner: the role of inhibition of Drp1 in ischemic brain damage, Neuropharmacology, 86 (2014) 103-115.

[40] G. Twig, O.S. Shirihai, The interplay between mitochondrial dynamics and mitophagy, Antioxidants & redox signaling, 14 (2011) 1939-1951.

[41] Y. Kageyama, M. Hoshijima, K. Seo, D. Bedja, P. Sysa-Shah, S.A. Andrabi, W. Chen, A. Hoke, V.L. Dawson, T.M. Dawson, K. Gabrielson, D.A. Kass, M. Iijima, H. Sesaki, Parkin-independent mitophagy requires Drp1 and maintains the integrity of mammalian heart and brain, The EMBO journal, 33 (2014) 2798-2813.

[42] P.I. Moreira, S.L. Siedlak, X. Wang, M.S. Santos, C.R. Oliveira, M. Tabaton, A. Nunomura, L.I. Szweda, G. Aliev, M.A. Smith, X. Zhu, G. Perry, Increased autophagic degradation of mitochondria in

Alzheimer disease, Autophagy, 3 (2007) 614-615.

국 문 초 록

아밀로이드 베타(Aβ)의 미토콘드리아 분절을 통한 신경세포 자멸사에서 Akt-Drp1 활성화의 역할

지도교수 한 호 재

서울대학교 대학원
수의학과 수의생명과학 전공
김 다 임

미토콘드리아의 형태적 변화와 그 기능은 긴밀히 연관되어 있으며, 미토콘드리아의 과도한 분절은 신경세포의 자멸사를 유도하여, 알츠하이머 질병을 일으키는 주요한 원인으로 보고되고 있다. 그러나 미토콘드리아 분절을 담당하는 주요 단백질인 Drp1이 어떠한 신호전달을 통해 활성화되는지는 현재까지 명확히 밝혀져 있지 않다. 이 연구에서는 미토콘드리아 분절과 신경세포의 자멸사 간의 연관성을 규명하고자 아밀로이드 베타(Aβ)에 의한 Drp1 인산화에 관련된 신호전달 기전을 조사하였다. Aβ가 미토콘드리아 형태변화와 Drp1 활성화에 미치는 영향은 공초점

현미경, 형태조절 단백질의 발현 및 면역침강법을 이용하여 분석하였다, Aβ에 의한 미토콘드리아 기능 변화는 활성산소 발생, 미토콘드리아 막전위($\Delta\Psi_m$) 변화 및 ATP 합성능력으로 평가하였으며, 세포 자멸사는 그 marker인 caspase-9/-3를 사용하여 확인하였다.

Aβ는 세포 내 칼슘 유입을 증가시켜 Akt 활성화를 통한 Drp1의 인산화를 증가시켰으며, 미토콘드리아 분절과 함께 capsase-9와 -3을 활성화시켰다. 그러나 Akt 억제제는 Drp1의 인산화를 감소시켜 미토콘드리아 분절을 차단함으로써, Akt가 Drp1의 세포질에서 미토콘드리아로의 이동을 조절함을 보여주었다. Aβ는 또한 활성산소 증가, 막전위($\Delta\Psi_m$) 감소 및 ATP 생성을 유의성 있게 감소시켰으나, 이는 Drp1 억제제인 mdivi-1로 처리하였을 때 차단되었다. Aβ에 의한 지속적인 Akt의 활성은 자가포식 기전을 억제함으로써 미토콘드리아 분절에 의한 기능손상을 악화시켰다. 그러나 자가포식 유도제인 Rapamycin 처리는 활성산소를 감소시켰다.

결론적으로 Aβ는 세포 내 칼슘 유입 증가로 Akt-Drp1의 인산화를 증가시킴으로써 mTOR를 통한 자가포식의 억제 및 미토콘드리아의 과도한 분절을 유발하여 신경세포의 자멸사를 일으켰다.

주요어: 아밀로이드 베타(Aβ), 미토콘드리아 다이나믹스(Mitochondrial dynamics), Akt, CaMKII, Drp1, 활성산소(ROS), 자가포식(Autophagy)
학번: 2014-21926